# DYNAMICS MODELING OF VARIABLE MASS SYSTEMS – A CASE STUDY OF AN UNDERWATER INERTIA BASED PROPELLED GLIDER PERFORMANCE

Zbigniew Kostka, Elżbieta Jarzębowska

*Warsaw University of Technology, Faculty of Power and Aeronautical Engineering, Warsaw, Poland*
*e-mail: zbigniew.kostka.dokt@pw.edu.pl; elzbieta.jarzebowska@pw.edu.pl*

Underwater gliders are autonomous underwater vehicles that are widely used in oceanography and coastal surveillance due to their low manufacturing costs and long operation time. This paper addresses the development of a dynamical model of such vehicles which are inertia propelled. The dynamical model is based upon the Boltzmann-Hamel equations modified to variable mass and inertia systems. It yields dynamics in a body-fixed frame using non-inertial coordinates. The theoretical development of the vehicle dynamics based upon the modified Boltzmann-Hamel equations is validated by the longitudinal dynamics model of the underwater glider and its performance resulted from the mass change.

*Keywords:* underwater gliders, AUV, variable-mass systems, Boltzmann-Hamel equations

## 1. Introduction

An underwater glider is a type of autonomous underwater vehicle (AUV) that is characterized by its specific way of propulsion. It changes its depth in water using different volume of the liquid in ballast tanks or an external blader. The net buoyancy or mass change is the factor that propels the glider forward. The greater the change from the equilibrium, the faster the vehicle traverses the given distance. Additionally, it is equipped with a moveable internal mass whose change of positions is used to enable vehicle turning. The vehicle thus characterizes by low manufacturing costs and exhibits long operation time. It can traverse thousands of kilometers during its mission as opposed to the range of a few kilometers by a typical vehicle with thrusters. Due to its characteristics, this class of underwater vehicles excels in oceanographic research (Rudnick, 2016), mostly in observation of oceanic fronts and water-mass properties, e.g. salinity or temperature (Wagawa *et al.*, 2020). It is also capable of long coastal surveillance missions, where its excels other underwater vehicles. The inertia based propelled underwater glider concept dates back to 1989, when Henry Stommel came up with an idea of a machine that operates without any external propulsion drives (Stommel, 1989). Then, many solutions came to life – starting from ALBAC (Kawaguchi *et al.*, 1995), the first prototype of a glider which could perform only one glide cycle. Next, three AUV's that share a very similar design: Slocum (Schofield *et al.*, 2007), Seaglider (Eriksen, 2001) and Spray (Rudnick *et al.*, 2016), were designed and built. There are also hybrid gliders which combine the attributes of the inertia based propelled glider and a non-inertially propelled one like Petrel (Wang *et al.*, 2011), Fölaga (Alvarez *et al.*, 2009) or blended body vehicle Zray (Brodsky and Luby, 2013). A different approach to the inertia based propelled system was adopted by Liquid Robotics, which developed a two-part system – a wave glider made of a surface float and an underwater glider (Hine *et al.*, 2009).

An inertia based propelled glider is a variable mass or buoyancy system that modifies its depth using different volume of the liquid in ballast tanks or in the external blader. The net buoyancy or mass change is the factor that propels the glider forward. The greater the change from the equilibrium, the faster the vehicle traverses the given distance. Moveable mass that may change its location inside the glider, is used to enable turning motions (Mahmoudian *et al.*, 2007). Hydrodynamic forces acting upon the glider are often calculated using the CFD approach (Sun *et al.*, 2021). They include lift, drag and the added mass calculations. However, the underwater gliders move slowly, and the classical hydrodynamics is enough to determine the forces and the Magnus effect is usually omitted due to its insignificance for slowly moving objects.

The most popular method to model underwater vehicle dynamics is the one based on Euler--Newton, which was used by Graver (2005) and Sun *et al.* (2023) or the Lagrange equations (Cruz, 2011) or fluid-multibody coupling (Wang *et al.*, 2023). Usually, the Lagrange based dynamics models use the Euler angles and they are equations in the body fixed frames identical to the flight dynamics models (Fossen, 1994). The dynamics model derivation based upon the Boltzmann--Hamel equations, which we present in the paper, is one of the most recent approaches that can be used to handle the variable mass system and be convenient for the controller design for the glider. The Boltzmann-Hamel equations were originally formulated for constant mass systems in non-inertial coordinates, often referred to as quasi-velocities, see e.g. (Neimark and Fufaev, 1972). Contrary to popular approaches like the Lagrange equations method, they are free of multipliers for constraints, which are incorporated into the equations of motion instead of being an additional algebraic relation (Müller, 2021). They enable handling nonholonomic systems due to arbitrary selection of quasi-velocities that may satisfy the nonholonomic constraints. There are a few examples of using the Boltzmann-Hamel equations approach to modelling and control of multibody systems, see e.g. (Jarzębowska, 2012). However, in the paper (Jarzębowska and Cichowski, 2018) the underwater vehicle dynamics is developed under some design and performance constraints that limit its usability, i.e. centers of masses are assumed to be in one axis and the change of position of the center of masses of ballast tanks are not taken into consideration.

In this paper, the concentricity of the centers of masses of the vehicle components and the center of buoyancy requirement was removed, and an additional parameter describing the position of the mass center of the ballast tank was added. To confirm the improvement of performance of the glider model with respect to performance of real gliders, simulation studies are presented. A longitudinal model of the glider has been derived and tested. The glider motion in the longitudinal plane is its typical motion, so it was selected for testing. A test that validates the propelling efficiency was performed using an open-loop control algorithm. The glider moved the so-called saw-tooth motion pattern, a traversal motion method that is typical for it in real-life motion scenarios. The control inputs and outputs were inspected and proposals for upgrading the performance through a targeted control strategy have been made. The contribution of this paper is the development of the modified Boltzmann-Hamel equations that account for the change of mass and inertia in the underwater vehicle. The model can have the constraints put upon the mass change. Assumptions about specific locations of $CB$ and $CG$ were removed, thus the dynamic model yields results closer to the reality. Based upon this framework, the longitudinal glider model is developed and validated.

The paper is organized as follows. After Introduction, Section 2 reports the Boltzmann-Hamel equations development for a constant mass system and presents their modification for variable mass systems. Section 3 details the underwater glider physical and dynamical models. Section 4 validates the glider dynamics and demonstrates its performance in longitudinal motion. The paper closes with conclusions, future research prospects and the list of references.

## 2. Boltzmann-Hamel equations for constant and variable mass systems

Boltzmann-Hamel equations originally developed for constant mass systems proved to be more efficient method of dynamics derivation for both holonomic and nonholonomic system models, the ones like underwater gliders, than the most widely used approaches like Newton-Euler or Lagrange equations. They are derived in quasi-velocities that represent velocities in a non-inertial, usually body fixed, reference frame. Due to the derivation method of the Boltzmann--Hamel equations and arbitrary selection of the quasi-velocities, the constraint equations can be taken as the quasi-velocities and, as such, incorporated into the system dynamics and reduce the size of the resulting system dynamics. In this Section we briefly report the derivation of the Boltzmann-Hamel equations. The detailed derivation and discussion of the equations can be found in e.g. (Neimark and Fufaev, 1972). Herein, we recall the development of the form of the equations as they were originally developed and we recall the concepts of quasi-velocities. These are needed to develop dynamics of the underwater vehicle.

The main motivation to reach for the Boltzmann-Hammel modeling method is that it proved to be effective in control applications for both unconstrained and constrained system models (Jarzębowska, 2012).

### 2.1. Quasi-velocities and generalized coordinates

Quasi-velocities $\omega_\sigma$ with $\sigma$ equal to the number of states can be selected arbitrarily as a linear or also as nonlinear combination of the generalized velocities $\dot{q}_i$ as in (2.1). Usually, they are the parameters associated with velocities in the body fixed frame, therefore they are referenced as non-inertial velocities

$$\omega_\sigma = a_{\sigma,0}(q) + \sum_{i=1}^{n} a_{\sigma,i}(q)\dot{q}_i \tag{2.1}$$

Quasi-coordinates are defined by their differentials as in (2.2). These terms are not integrable, therefore the parameters $\pi_\sigma$ do not exist physically. If relations (2.2) can be integrated, then they are generalized velocities, whose derivatives can also serve as quasi-velocities.

$$d\pi_\sigma = a_{\sigma,0}(q)dt + \sum_{i=1}^{n} a_{\sigma,i}(q)dq_i \tag{2.2}$$

Usually, for selection of quasi-velocities we assume that $a_{\sigma,0}(q) = 0$, so expression (2.1) can be rewritten as $(2.3)_1$. Assuming that relations $(2.3)_1$ are invertible, the generalized velocities can be presented as linear combinations of quasi-velocities $(2.3)_2$. Based upon (2.2) and $(2.3)_2$, relation $(2.3)_3$ can be written. Combining expressions $(2.3)_{1,2}$, we can determine relations (2.4) between the coefficients $a_{l,\sigma}$ and $b_{\sigma,j}$

$$\omega_\sigma = \sum_{i=1}^{n} a_{\sigma,i}(q)\dot{q}_i \qquad \dot{q}_\sigma = \sum_{j=1}^{n} b_{\sigma,j}(q)\omega_j \qquad \delta q_\sigma = \sum_{j-1}^{n} b_{\sigma,j}(q)\delta\pi_j \tag{2.3}$$

and

$$\sum_{\sigma=1}^{n} a_{l,\sigma} b_{\sigma,j} = \delta_{l,j} = \begin{cases} 1 & \text{for} \quad l = j \\ 0 & \text{for} \quad l \neq j \end{cases} \tag{2.4}$$

In the case of the $m$ nonholonomic constraint equations imposed upon a system, relations (2.3) consist of $m$ quasi-velocities identically satisfying the constraint equations, and the rest $(n - m)$ of quasi-velocities are selected arbitrarily, which is practically suitable to the considered system modling.

### 2.2. The Boltzmann-Hamel equations for constant mass systems

The Boltzmann-Hamel equations can be derived, roughly speaking, from Lagrange equations $(2.5)_1$, where the generalized coordinates are replaced by quasi-velocities (2.1) and quasi-coordinates (2.2). The Lagrange equations, assuming independent $\delta q_\sigma$ $(2.5)_1$ can be presented as in $(2.5)_2$

$$
\begin{aligned}
&\sum_{\sigma=1}^{n}\Big[\frac{d}{dt}\Big(\frac{\partial T}{\partial \dot{q}_\sigma}\Big) - \frac{\partial T}{\partial q_\sigma} - Q_\sigma\Big]\delta q_\sigma = 0 \\
&\sum_{\sigma=1}^{n}\frac{d}{dt}\Big(\frac{\partial T}{\partial \dot{q}_\sigma}\Big)b_{\sigma,j} - \sum_{\sigma=1}^{n}\frac{\partial T}{\partial q_\sigma}b_{\sigma,j} = \sum_{\sigma=1}^{n}Q_\sigma b_{\sigma,j}
\end{aligned}
\tag{2.5}
$$

After denoting the kinetic energy written in quasi-velocities as $T^*$ and taking into account $(2.3)_2$, a relation between $T^*(\omega, q, t)$ and $T(\dot{q}, q, t)$ can be derived as in $(2.6)_1$. Relation $(2.6)_1$ is then used in transformations of the first term of $(2.5)_2$. It yields $(2.6)_2$

$$
\begin{aligned}
&\frac{\partial T^*}{\partial \omega_j} = \sum_{\sigma=1}^{n}\frac{\partial T}{\partial \dot{q}_\sigma}\frac{\partial \dot{q}_\sigma}{\partial \omega_j} = \sum_{\sigma=1}^{n}\frac{\partial T}{\partial \dot{q}_\sigma}b_{\sigma,j} \\
&\sum_{\sigma=1}^{n}\frac{d}{dt}\Big(\frac{\partial T}{\partial \dot{q}_\sigma}\Big)b_{\sigma,j} = \frac{d}{dt}\sum_{\sigma=1}^{n}\frac{\partial T}{\partial \dot{q}_\sigma}b_{\sigma,j} - \sum_{\sigma=1}^{n}\frac{\partial T}{\partial \dot{q}_\sigma}\frac{\partial b_{\sigma,j}}{\partial t} = \frac{d}{dt}\Big(\frac{\partial T^*}{\partial \omega_j}\Big) \\
&\quad + \sum_{\sigma=1}^{n}\sum_{l=1}^{n}\sum_{\lambda=1}^{n}\sum_{\alpha=1}^{n}\frac{\partial T^*}{\partial \omega_l}\omega_\alpha\frac{\partial a_{l,\sigma}}{\partial q_\lambda}b_{\sigma,j}b_{\lambda,\alpha}
\end{aligned}
\tag{2.6}
$$

The derivative of $T$ with respect to generalized coordinates can be expanded as in $(2.7)_1$. It is then used for transformation of the second term of $(2.5)_2$ and it results in $(2.7)_2$

$$
\begin{aligned}
&\frac{\partial T}{\partial q_\sigma} = \frac{\partial T^*}{\partial q_\sigma} + \sum_{l=1}^{n}\frac{\partial T^*}{\partial \omega_l}\frac{\partial \omega_l}{\partial q_\sigma} = \frac{\partial T^*}{\partial q_\sigma} + \sum_{l=1}^{n}\sum_{\lambda=1}^{n}\sum_{\alpha=1}^{n}\frac{\partial T^*}{\partial \omega_l}\frac{\partial a_{l,\lambda}}{\partial q_\sigma}b_{\lambda,\alpha}\omega_\alpha \\
&\sum_{\sigma=1}^{n}\frac{\partial T}{\partial q_\sigma}b_{\sigma,j} = \frac{\partial T^*}{\partial \pi_j} + \sum_{\sigma=1}^{n}\sum_{l=1}^{n}\sum_{\lambda=1}^{n}\sum_{\alpha=1}^{n}\frac{\partial T^*}{\partial \omega_l}\frac{\partial a_{l,\lambda}}{\partial q_\sigma}b_{\lambda,\alpha}\omega_\alpha b_{\sigma,j}
\end{aligned}
\tag{2.7}
$$

The right hand side term in $(2.5)_2$ is rewritten as $(2.8)_1$, and $Q_j^*$ is the generalized force related to quasi-velocity $\omega_j$. Relations $(2.6)_1$, $(2.7)_1$ and $(2.8)_1$ when inserted into $(2.5)_2$ result in equation $(2.8)_2$

$$
\begin{aligned}
&Q_j^* = \sum_{\sigma=1}^{n}Q_\sigma b_{\sigma,j} \\
&\frac{d}{dt}\Big(\frac{\partial T^*}{\partial \omega_j}\Big) - \frac{\partial T^*}{\partial \pi_j} + \sum_{\alpha=1}^{n}\sum_{l=1}^{n}\frac{\partial T^*}{\partial \omega_l}\omega_\alpha\sum_{\sigma=1}^{n}\sum_{\lambda=1}^{n}\Big(\frac{\partial a_{l,\sigma}}{\partial q_\lambda} - \frac{\partial a_{l,\lambda}}{\partial q_\sigma}\Big)b_{\sigma,j}b_{\lambda,\alpha} = Q_j^*
\end{aligned}
\tag{2.8}
$$

After introducing the so called Boltzmann-Hamel coefficients $(2.9)_1$, equation $(2.8)_2$ can be presented as $(2.9)_2$

$$
\begin{aligned}
&\gamma_{j\alpha}^{l} = \sum_{\sigma=1}^{n}\sum_{\lambda=1}^{n}\Big(\frac{\partial a_{l,\sigma}}{\partial q_\lambda} - \frac{\partial a_{l,\lambda}}{\partial q_\sigma}\Big)b_{\sigma,j}b_{\lambda,\alpha} \\
&\frac{d}{dt}\Big(\frac{\partial T^*}{\partial \omega_j}\Big) - \frac{\partial T^*}{\partial \pi_j} + \sum_{\alpha=1}^{n}\sum_{l=1}^{n}\gamma_{j\alpha}^{l}\frac{\partial T^*}{\partial \omega_l}\omega_\alpha = Q_j^*
\end{aligned}
\tag{2.9}
$$

The third term of equation $(2.9)_2$ can be further simplified, i.e. writing the Boltzmann-Hammel coefficients into a matrix form $(2.10)_1$ we can obtain a single sum as $(2.10)_2$. Recalling that the

quasi-velocity vector is $(n \times 1)$ dimensional, the final form of equation $(2.9)_2$ can be presented as $n$ equations $(2.10)_3$ referred to as the Boltzmann-Hamel equations

$$
\begin{aligned}
\boldsymbol{\Gamma}_\alpha &= \begin{bmatrix} \gamma_{1\alpha}^1 & \gamma_{1\alpha}^2 & \cdots & \gamma_{1\alpha}^n \\ \gamma_{2\alpha}^1 & \gamma_{2\alpha}^2 & \cdots & \gamma_{2\alpha}^n \\ \vdots & \vdots & \vdots & \ddots \\ \gamma_{n\alpha}^1 & \gamma_{n\alpha}^2 & \cdots & \gamma_{n\alpha}^n \end{bmatrix} \\
\mathbf{G}(\boldsymbol{\omega}) &= \sum_{\alpha=1}^n \boldsymbol{\Gamma}_\alpha \omega_\alpha \\
\frac{d}{dt}\Big(\frac{\partial T^*}{\partial \boldsymbol{\omega}}\Big) &- \frac{\partial T^*}{\partial \boldsymbol{\pi}} + \mathbf{G}(\boldsymbol{\omega})\frac{\partial T^*}{\partial \boldsymbol{\omega}} = \mathbf{Q}^*
\end{aligned}
\tag{2.10}
$$

### 2.3. Boltzmann-Hamel equations for variable-mass systems

The original Boltzmann-Hamel equations cannot be directly applied to derive dynamical models of variable mass and variable inertia systems. Therefore, some modifications are needed. The kinetic energy of the system written in quasi-velocities depends on the form of the inertia matrix $\mathbf{M}$ (2.11). It is time dependent or may also depend upon other parameters, e.g. velocity, if mass or inertia are prescribed to change according to some constraint equations. It impacts the form of equations $(2.10)_3$.

In this Section, we present a modification of the Boltzmann-Hamel equations to encompass the mass and inertia changes. The main idea is to explicitly account for the change of mass of water in the vehicle water tanks and motion the movable mass. The need of doing so is to obtain an explicit exposition of these terms in the system dynamical equations. This in turn is essential for a design of the control system. In this paper, we design a feedforward controller only to regulate mass of water in the water tank, however, the future work aims at the design of feedback control for both the regulation of water amount and for movable mass motion. Control of the movable mass is essential for performing maneuvers by the vehicle. Concluding then, the dynamic underwater vehicle model which we present herein will be transformed into a dynamic control model with the control inputs being the change of mass of water in the water tank and the positions of the movable mass.

To develop the variable inertia dynamics, we assume a modified form of the inertia matrix that includes explicitly a time derivative of the $\mathbf{M}$ in (2.11)

$$
\frac{d}{dt}\Big(\frac{\partial T^*}{\partial \boldsymbol{\omega}}\Big) = \mathbf{M}(\dot{\boldsymbol{\omega}}) + \dot{\mathbf{M}}\boldsymbol{\omega}
\tag{2.11}
$$

Thus the variable mass and inertia Boltzmann-Hamel equations can be written in a compact form

$$
\mathbf{M}(\dot{\boldsymbol{\omega}}) + \dot{\mathbf{M}}\boldsymbol{\omega} - \frac{\partial T^*}{\partial \boldsymbol{\pi}} + \mathbf{G}(\boldsymbol{\omega})\frac{\partial T^*}{\partial \boldsymbol{\omega}} = \mathbf{Q}^*
\tag{2.12}
$$

Equation (2.12) is applied to develop dynamical equations of the longitudinal motion for the underwater vehicle model.

## 3. Dynamics model of the underwater glider

To validate dynamics of the variable inertia system (2.13), this Section presents development of a longitudinal model of the underwater glider to confirm its saw-tooth motion pattern and tests through simulations the inertia based propelling efficiency using an open-loop controller. The

longitudinal motion is a dominant one in real gliders so it can be taken for model validation. The glider saw-tooth motion pattern is a traversal method which is typical in real-life scenarios. The control inputs and outputs were inspected and propositions for upgrading the performance through a targeted control strategy have been made.

In this paper, we adopt the assumption about the design of a typical underwater glider. In contrary to (Jarzębowska and Cichowski, 2018), an assumption about concentricity of centers of masses of the vehicle components and the center of buoyancy were removed, and an additional parameter describing the position of the mass center of the ballast tank was added. The underwater glider is assumed to be composed of two main components: a hull and a ballast tank. The buoyancy center ($CB$) of the hull is the same as the $CB$ of the whole system, but its mass center ($CM$) does not coincide with the center of mass of the vehicle. The other mentioned components are treated as point masses

$$M = m_h + m_{tank} \tag{3.1}$$

The movable mass is not present in our model, since it is installed for the space maneuvers of the glider. Also, the second general assumption is that we do not assume that all vehicle components are located along the vehicle longitudinal axis, i.e. they can be displaced from $x$ axis; see Fig. 1. Additionally, the location of the $CM$ of the ballast tank changes according to the change of mass of the liquid rested in it. One more assumption enables positioning the $CM$ of the vehicle below its $CB$, thus increasing its stability. All these assumptions make our glider model close to real designs of such kind of vehicles.
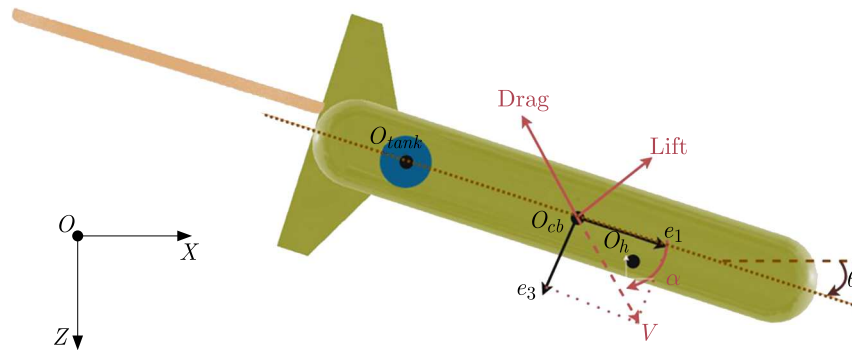


Fig. 1. A glider model and its components

Calculations which we present are performed in two reference frames: inertial and the body frame. The $z$ and $e_3$ axes point downward instead of upward, as it is traditionally assumed in many works. The change was done to emphasize that the glider moves below the water surface. The glider model is presented in Fig. 1 and the data representing its parameters are shown in Table 1.

To describe the glider longitudinal motion, a state vector consists of 3 quasi-velocities and 2 generalized velocities $(3.2)_3$ and $(3.2)_4$. The quasi-velocities are the linear velocities along the body axis $e_1$, $e_3$, and $Q$ refers for the pitch angle. Notice, that $Q$ is the generalized velocity adopted as the quasi-velocity. The generalized velocities are derivatives of the position coordinates along inertia axes $x$ and $z$ $(3.2)_2$. Equations $(3.2)_5$ and $(3.2)_6$ present transformations between the quasi-velocities and generalized velocities

**Table 1.** Glider data

| Parameter | Significance |
|---|---|
| $m_h = 26.9\,\text{kg}$ | mass of the hull |
| $z_{CB,tank} = 0\,\text{m}$ | $z$ position of $CM$ of ballast tank with respect to $CB$ of the glider |
| $x_{CB,h} = 0\,\text{m}$ | $x$ position of $CM$ of hull with respect to $CB$ of the glider |
| $z_{CB,h} = 0.1\,\text{m}$ | $z$ position of $CM$ of hull with respect to $CB$ of the glider |
| $g = 9.81\,\text{m/s}^2$ | acceleration due to gravity |
| $v = 0.0274\,\text{m}^3$ | volume of glider |
| $\rho = 1023.6\,\text{kg/m}^3$ | density of seawater |
| $K_{D0} = 7.19\,\text{kg/m}$ | hydrodynamic constant impacting linear velocity $U$ |
| $K_D = 386.29\,\text{kg/(m·rad}^2)$ | hydrodynamic constant associated with square of $\alpha$ impacting linear velocity $U$ |
| $K_\alpha = 440.99\,\text{kg/(m·rad)}$ | hydrodynamic constant associated with $\alpha$ impacting linear velocity $W$ |
| $K_M = 65.84\,\text{kg/rad}$ | hydrodynamic constant associated with $\alpha$ impacting angular velocity $Q$ |
| $K_Q = 205.64\,\text{kg·s/rad}^2$ | hydrodynamic constant associated with angular velocity $Q$ impacting $Q$ |
| $I_{CM,h} = 5.919\,\text{kg·m}^2$ | moment of inertia of hull |

$$
\boldsymbol{\omega}_v = \begin{bmatrix} U \\ W \end{bmatrix} \qquad \dot{\mathbf{q}}_v = \begin{bmatrix} \dot{x}_{CB} \\ \dot{z}_{CB} \end{bmatrix}
$$

$$
\boldsymbol{\omega}^{\mathrm{T}} = \begin{bmatrix} \omega_v^{\mathrm{T}} & Q & \dot{x}_{CB,tank}^{\mathrm{T}} \end{bmatrix} \qquad \dot{\mathbf{q}}_v^{\mathrm{T}} = \begin{bmatrix} \dot{q}_v^{\mathrm{T}} & \dot{\theta} & \dot{x}_{CB,tank}^{\mathrm{T}} \end{bmatrix} \tag{3.2}
$$

$$
\boldsymbol{\omega}_v = \begin{bmatrix} U \\ W \end{bmatrix} = \begin{bmatrix} \cos\theta & -\sin\theta \\ \sin\theta & \cos\theta \end{bmatrix} \begin{bmatrix} \dot{x}_{CB} \\ \dot{z}_{CB} \end{bmatrix} = \boldsymbol{\Lambda}_v \dot{\overline{\mathbf{q}}}_v \qquad Q = \dot{\theta}
$$

The model of the glider was created with the use of the Boltzmann-Hamel equations for variable inertia (2.12). Due to the change of mass in the ballast tank, the mass $M$ and the position of the $CM$ of the whole glider with respect to its $CB$ $\mathbf{r}_{CB,CM}$ is depicted by $(3.3)_1$ and the inertia matrix $\mathbf{M}$ of the system are both time-dependent. The moment of inertia $(3.3)_2$ includes the moment of inertia of the hull $I_{CM,h}$, masses of the ballast tank $m_{tank}$ and hull $m_h$ as well as the positions of the $CM$ of the hull $r_{CB,h}$ and of the ballast tank $\mathbf{r}_{CB,tank}$ $(3.3)_3$ with respect to the $CB$ of the glider. They are all time-dependent. Therefore, inertia matrix of the glider $(3.3)_4$ depends not only on the position changes of the mass centers, but also on the change of mass in the ballast tank

$$
\mathbf{r}_{CB,CM} = \begin{bmatrix} x_{CB,CM} \\ z_{CB,CM} \end{bmatrix}
$$

$$
I = I_{CM,h} + n_{tank} r_{CB,tank}^{\mathrm{T}} r_{CB,tank} + m_h r_{CB,h}^{\mathrm{T}} r_{CB,h}
$$

$$
\mathbf{r}_{CB,tank} = \begin{bmatrix} x_{CB,tank} \\ z_{CB,tank} \end{bmatrix} \tag{3.3}
$$

$$
T = \frac{1}{2}\overline{\boldsymbol{\omega}}^{\mathrm{T}} \begin{bmatrix} M & 0 & Mz_{CB,CM} & m_{tank} \\ 0 & M & -Mx_{CB,CM} & 0 \\ Mz_{CB,CM} & -Mx_{CB,CM} & I & m_{tank}z_{CB,tank} \\ m_{tank} & 0 & m_{tank}z_{CB,tank} & m_{tank} \end{bmatrix} \overline{\boldsymbol{\omega}} = \frac{1}{2}\overline{\boldsymbol{\omega}}^{\mathrm{T}}\mathbf{M}\overline{\boldsymbol{\omega}}
$$

Three external forces act upon the glider model $(3.4)_1$. They are gravity $(3.4)_2$, buoyancy $(3.4)_3$ and hydrodynamic forces $(3.4)_4$. The hydrodynamic forces account only for a normalized drag and lift. The added mass effect and the Magnus effect are excluded from the calculations. The Magnus effect is irrelevant due to small velocity of the glider. The added mass effect is assumed to be constant for a specific pitch angle. The hydrodynamic forces are transformed to the body-fixed frame from the non-inertial wind frame using the attack angle $\alpha$ $(3.5)_1$ and the total velocity of the vehicle $V_0$ $(3.5)_2$

$$\mathbf{F}_{ext} = \mathbf{F}_{G,CB} + \mathbf{F}_{B,CB} + \mathbf{F}_{H,CB}$$

$$\mathbf{F}_{G,CB} = \begin{bmatrix} \cos\theta & -\sin\theta \\ \sin\theta & \cos\theta \\ z_{CB,CM}\cos\theta & x_{CB,CM}\sin\theta \\ 0 & 0 \end{bmatrix} \begin{bmatrix} 0 \\ Mg \end{bmatrix}$$

$$\mathbf{F}_{B,CB} = \begin{bmatrix} \mathbf{1}_{2\times2} & \mathbf{0}_{2\times2} \\ \mathbf{0}_{2\times2} & \mathbf{0}_{2\times2} \end{bmatrix} \begin{bmatrix} \mathbf{\Lambda} \\ \mathbf{0}_{2\times2} \end{bmatrix} \begin{bmatrix} 0 \\ -\rho v g \end{bmatrix} \tag{3.4}$$

$$\mathbf{F}_{H,CB} = \begin{bmatrix} \cos\alpha & -\sin\alpha & 0 & 0 \\ \sin\alpha & \cos\alpha & 0 & 0 \\ 0 & 0 & 1 & 0 \\ 0 & 0 & 0 & 0 \end{bmatrix} \begin{bmatrix} -K_{D0} - K_D(\alpha^2) \\ -K_\alpha \alpha \\ -K_M\alpha - K_Q Q \\ 0 \end{bmatrix} V_0^2$$

and

$$\alpha = \arctan 2(W, U) \qquad V_0 = \sqrt{U^2 + W^2} \tag{3.5}$$

## 4. Simulation of the saw-tooth motion of the underwater glider

The so called saw-tooth motion is a typical motion of an inertia-propelled underwater vehicle. In this Section we develop the longitudinal dynamics model of the vehicle and validate its performance. Specifically, the model validates the self-propelling capabilities of the vehicle due to the change of its mass and inertia. The underwater vehicle increases its net weight when it is close to the surface and reduces it at the maximum desired depth. The cycle repeats throughout the entire operation. The bigger the net weight change, the faster the vehicle moves. The mass change is achieved through changes of the mass or volume of the liquid in the ballast tank. The process occurs near the surface or at the maximum depth only, therefore the inertia propelled glider is much more energy efficient than the one equipped with other propulsion means like thrusters, which need a constant influx of energy to keep floating and moving forward.

During the simulation studies, an open-loop control algorithm was used to execute forward motion by the saw-tooth pattern. Using the open-loop control, we get an insight into the glider dynamics with respect to the future feedback control design. In the simulation study, there was one control input, i.e. the mass change in the ballast tank. The mass of water in the tank changes between 0.56 kg and 2.2 kg as seen in Fig. 2a. The resulting saw-tooth motion is shown in Fig. 2b. The kind of periodicity of the saw-tooth motion pattern depends on how fast is the change of water amount in the water tanks. Initial values for quasi-velocities were set to $U_0 = 0.5$ m/s and $W_0 = 0.25$ m/s.

The underwater glider controlled by the control input function shown in Fig. 2a is able to achieve approximately constant velocity. The small velocity deviations came from the net weight change process at the surface or the maximum depth and a slight difference of the absolute value of the net weight during sinking and surfacing. The traversal distance in the $x$ direction in time is shown in Fig. 3a, while depth in time is in Fig. 3b.
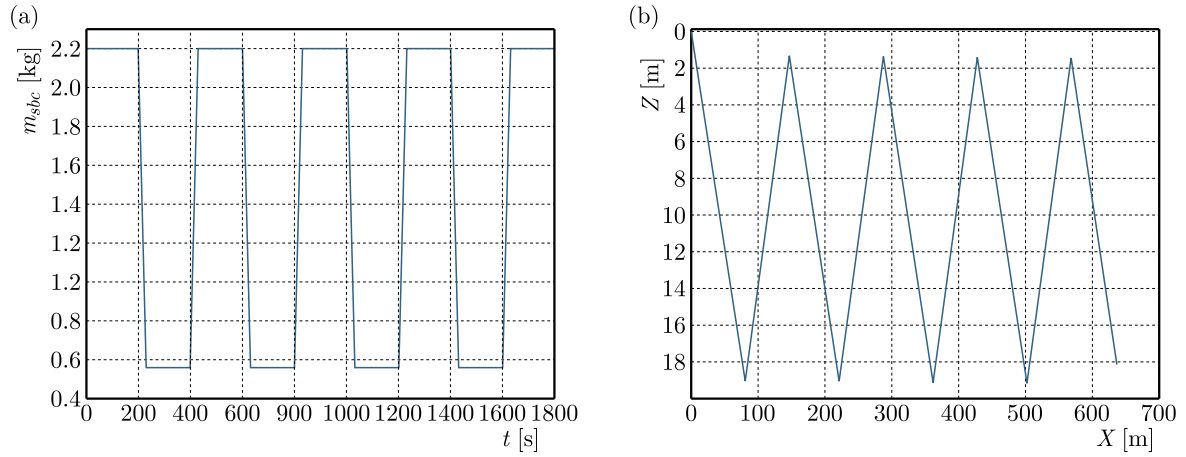
(a)



(b)



Fig. 2. (a) Control input time history for saw-tooth motion – mass change in the front ballast tank. (b) Saw-tooth trajectory pattern of the underwater glider
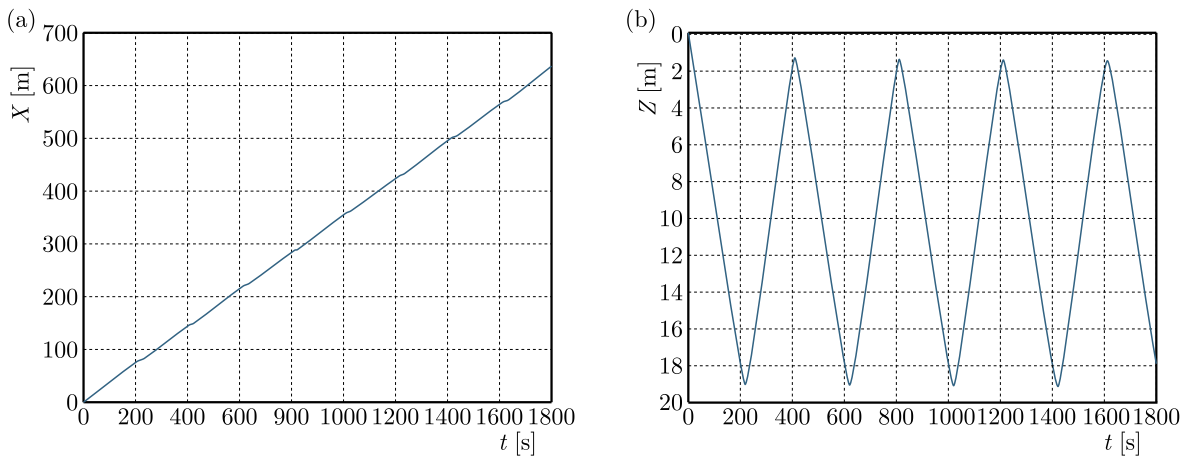
(a)



(b)



Fig. 3. (a) The traversal distance in the $x$ direction in time covered by the glider. (b) The vertical distance in the $z$ direction in time covered by the glider

The angle in the longitudinal motion that changed in time was the pitch angle. The changes of the pitch angle in time are presented in Fig. 4. The pitch angle initial value is set to be equal to $\pi/8$.
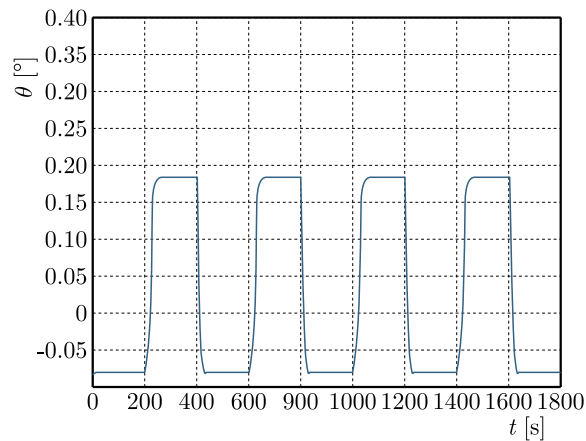


Fig. 4. The changes of the underwater glider pitch angle in time

## 5.    Conclusion and perspective

The problem of modeling of the underwater glider dynamics is addressed in the paper with the aid of the Boltzmann-Hamel equations modified to encompass variable mass and inertia of the system. The modified Boltzmann-Hamel equations can serve for modeling of a system with any desired change of mass in water tanks and any motion of a movable mass that enables vehicle turning maneuvers.

In our modeling approach, the constraints that are assumed as in many references, i.e. concentricity of mass centers of the glider body components and the buoyancy center, and no influence of the change of mass on the location of the mass center of the ballast tank were relaxed.

The advantages of the modified modeling approach may serve both for modeling of constrained variable mass underwater vehicles, including constraints on the mass change, and for simplifing control applications like moving along desired trajectories or controling the mass change required for some maneuvers.

The presented dynamics model still requires some extensions, specifically as it is intended to be used for control applications. For example, it would need more precise calculation of hydrodynamic forces acting upon the vehicle. Future research aims at calculating the forces using the CFD method to get results closer to real ones than simplified outcomes in form of constant values for a specific attack angle what is often assumed in many references.

## References

1. ALVAREZ A., CAFFAZ A., CAITI A., CASALINO G., GUALDESI L., *et al.*, 2009, Fòlaga: a low-cost autonomous underwater vehicle combining glider and AUV capabilities, *Ocean Engineering*, **36**, 1, 24-38

2. BRODSKY P., LUBY J., 2013, *Flight Software Development for the Liberdade Flying Wing Glider*, Office of Naval Research, Arlington

3. CRUZ N. (ED.), 2011, *Autonomous Underwater Vehicles*, InTech, DOI: 10.5772/923

4. ERIKSEN C.C., OSSE T.J., LIGHT R.D., WEN T., LEHMAN T.W., *et al.*, 2001, Seaglider: a long-range autonomous underwater vehicle for oceanographic research, *IEEE Journal of Oceanic Engineering*, **26**, 4, 424-436

5. FOSSEN T.I., 1994, *Guidance and Control of Ocean Vehicles*, 1st ed., Wiley

6. GRAVER J.G., 2005, Underwater gliders: dynamics, control and design, Ph.D. Thesis, Princeton University, Princeton

7. HINE R., WILLCOX S., HINE G., RICHARDSON T., 2009, The wave glider: a wave-powered autonomous marine vehicle, *Oceans 2009, IEEE Conference*, 1-6

8. JARZĘBOWSKA E., 2012, *Model-Based Tracking Control of Nonlinear Systems*, CRC Series: Modern Mechanics and Mathematics, CRC Press, Taylor & Francis Group, Boca Raton

9. JARZĘBOWSKA E., CICHOWSKI M., 2018, Dynamics modeling and performance analysis of underwater vehicles based on the Boltzmann-Hamel equations approach, *MATEC Web of Conferences*, **148**, 03005

10. KAWAGUCHI K., URA T., ORIDE M., SAKAMAKI T., 1995, Development of shuttle type AUV "ALBAC" and sea trials for oceanographic measurement, *Journal of the Society of Naval Architects of Japan*, **178**, 657-665

11. MAHMOUDIAN N., GEISBERT J., WOOLSEY C., 2007, *Dynamics and Control of Underwater Gliders I: Steady Motions*, Virginia Center for Autonomous Systems, Blacksburg, Virginia

12. Mahmoudian N., Geisbert J., Woolsey C., 2010, *Dynamics and Control of Underwater Gliders II: Steady Motions*, Virginia Center for Autonomous Systems, Blacksburg, Virginia

13. Müller A., 2021, On the Hamel coefficients and the Boltzmann-Hamel equations for the rigid body, *Journal of Nonlinear Science*, **31**, 2, 40

14. Neimark J.I., Fufaev N.A., 1972, *Dynamics of Nonholonomic Systems*, American Mathematical Society, Providence, RI

15. Rudnick D.L., 2016, Ocean research enabled by underwater gliders, *Annual Review of Marine Science*, **8**, 519-541

16. Rudnick D.L., Davis R.E., Sherman J.T., 2016, Spray Underwater Glider Operations, *Journal of Atmospheric and Oceanic Technology*, **33**, 6, 1113-1122

17. Schofield O., Kohut J., Aragon D., Creed L., Graver J., *et al.*, 2007, Slocum gliders: robust and ready, *Journal of Field Robotics*, **24**, 6, 473-485

18. Stommel H., 1989, The slocum mission, *Oceanography*, **2**, 1, 22-25

19. Sun C., Tian J., Huang R., Dong H., Li H., Ma Y., 2023, Internal layout optimization of the blended-wing-body underwater glider based on a range target, *Ocean Engineering*, **280**, 114450

20. Sun W., Zang W., Liu C., Guo T., Nie Y., Song D., 2021, Motion pattern optimization and energy analysis for underwater glider based on the multi-objective artificial bee colony method, *Journal of Marine Science and Engineering*, **9**, 3, 327

21. Wagawa T, Kawaguchi Y., Igeta Y., Honda N., Okunishi T., Yabe I., 2020, Observations of oceanic fronts and water-mass properties in the central Japan Sea: Repeated surveys from an underwater glider, *Journal of Marine Systems*, **201**, 103242

22. Wang H., Chen J., Feng Z., Li Y., Deng C., Chang Z., 2023, Dynamics analysis of underwater glider based on fluid-multibody coupling model, *Ocean Engineering*, **278**, 114330

23. Wang S., Sun X., Wang Y., Wu J., Wang X., 2011, Dynamic modeling and motion simulation for a winged hybrid-driven underwater glider, *China Ocean Engineering*, **25**, 1, 97-112

24. Zhang S., Yu J., Zhang A., Zhang F., 2013, Spiraling motion of underwater gliders: Modeling, analysis, and experimental results, *Ocean Engineering*, **60**, 1-13